Research Article

Journal of Molecular Recognition

Received: 7 November 2008, Revised: 7 March 2009, Accepted: 16 March 2009, Published online in Wiley InterScience: 28 April 2009

(www.interscience.wiley.com) DOI:10.1002/jmr.955

Atomic force microscopy study of the role of LPS O-antigen on adhesion of *E. coli*

Joshua Strauss[a], Nancy A. Burnham[b] and Terri A. Camesano[a]*

The O-antigen is a highly variable component of the lipopolysaccharide (LPS) among *Escherichia coli* strains and is useful for strain identification and assessing virulence. While the O-antigen has been chemically well characterized in terms of sugar composition, physical properties such as O-antigen length of *E. coli* LPS have not been well studied, even though LPS length is important for determining binding of bacteria to biomolecules and epithelial cells. Atomic force microscopy (AFM) was used to characterize the physicochemical properties of the LPS of eight *E. coli* strains. Steric repulsion between the AFM tip (silicon nitride) and the *E. coli* cells was measured and modeled, to determine LPS lengths for three O157 and two O113 *E. coli* strains, and three control (K12) strains that do not express the O-antigen. For strains with an O-antigen, the LPS lengths ranged from 17 ± 10 to 37 ± 9 nm, and LPS length was positively correlated with the force of adhesion (F_{adh}). Longer lengths of LPS may have allowed for more hydrogen bonding between the O-antigen and silanol groups of the AFM silicon nitride tip, which controlled the magnitude of F_{adh}. For control strains, LPS lengths ranged from 3 ± 2 to 5 ± 3 nm, and there was no relationship between LPS length and adhesion force between the bacterium and the silicon nitride tip. In the absence of the O-antigen, we attributed F_{adh} to electrostatic interactions with lipids in the bacterial membrane. Copyright © 2009 John Wiley & Sons, Ltd.

Keywords: *E. coli*; bacterial adhesion; AFM; LPS; O-antigen; adhesion force

INTRODUCTION

Recent *E. coli* outbreaks in spinach and meat have demonstrated the continuing threats posed by pathogenic *E. coli* (Strachan *et al.*, 2006; Ciftcioglu *et al.*, 2008; Uhlich *et al.*, 2008). However, in nature, most *E. coli* are harmless and many are necessary for human digestion (Bettelheim *et al.*, 1974). Testing for pathogenic *E. coli* includes serotyping of the O-antigen. *E. coli* serotypes O157 and O113 usually cause severe symptoms of dysentery and can lead to kidney failure (Griffin and Tauxe, 1991; Dean-Nystrom *et al.*, 1997; Nataro and Kaper, 1998; Parma *et al.*, 2000). O-antigen is an important indicator for determining if an isolated *E. coli* strain is pathogenic, however, there are no universal relationships between serotype and pathogenicity. The most problematic foodbourne pathogen is *E. coli* O157, which is synonymous with widespread outbreaks of contaminated food (Besser *et al.*, 1993; Bell *et al.*, 1994; Maki, 2006). While the O-antigen is known to be important for *E. coli* pathology, the evolutionary advantage of the numerous variations of O-antigens remains unclear.

The LPS is comprised of the lipid A that extends from the bacterial membrane, followed by an inner and outer core, and a repeating O-antigen chain (Hitchcock *et al.*, 1986; Goldman and Hunt, 1990; Caroff and Karibian, 2003). The lipid A contains saturated fats and phospholipids, which in part gives the bacterium a negative charge (Caroff and Karibian, 2003) and is widely conserved among *E. coli* (Sumihiro Hase, 1976; Schromm *et al.*, 2000). Serotyping identifies *E. coli* in terms of the O-antigen, flagella antigen, and capsular antigen (Hitchcock *et al.*, 1986). The O-antigen is a polysaccharide with repeating units of 1 to >100 (Franco *et al.*, 1998; Murray *et al.*, 2006). The O-antigens of >180 *E. coli* strains have been chemically characterized (Stenutz *et al.*, 2008). Rough bacteria are common laboratory strains that lack the O-antigen. Smooth strains are the most commonly *E. coli* found in nature, which express repeating O-antigen units (Whitfield, 1995).

The LPS core and O-antigen are key components that mediate bacterial binding with inorganic materials such as silicon nitride (Abu-Lail and Camesano, 2003b) and enable aggregation with other cells (Sheng *et al.*, 2008). The O-antigen assists *E. coli* adhesion through hydrogen binding (Tomme *et al.*, 1996). The length of the O-antigen may control bacterial interaction with biomolecules and other cells (Tang *et al.*, 2007).

Silicon nitride is a model material to analyze O-antigen bonding since silica will form on the surface of the silicon nitride following oxidation (Riley, 2000). Silica is coated with silanol and binds to the O-antigen via hydroxyl groups (Zhuravlev, 1987). A previous study demonstrated that bonding of bacterial O-antigens to silanol occurred via hydrogen bonding (Jucker *et al.*, 1997). Due to its larger size, the O-antigen likely masks interactions of the lipid A and underlying proteins from solid surfaces (Makin and Beveridge, 1996), thus the O-antigen may control bacterial adhesion for smooth strains.

The AFM is an innovative tool for measuring molecular–molecular interaction forces (Liu *et al.*, 2008) and capturing high

* *Correspondence to: T. A. Camesano, Department of Chemical Engineering, Life Science and Bioengineering Center at Gateway Park, 100 Institute Rd., Worcester, MA 10609, USA.*
E-mail: terric@wpi.edu

a *J. Strauss, T. A. Camesano*
Department of Chemical Engineering, Worcester Polytechnic Institute, Worcester, MA 01609, USA

b *N. A. Burnham*
Department of Physics, Worcester Polytechnic Institute, Worcester, MA 01609, USA

resolution images (Karrasch *et al.*, 1994; Moller *et al.*, 1999; Touhami *et al.*, 2003). Bacterial samples require little preparation before examination with AFM. AFM steric modeling has been used extensively to calculate the thickness of bacterial surface molecules and measure the effects of solution ionic strength on polysaccharides (Camesano and Logan, 2000; Taylor and Lower, 2008). Previous studies have not systemically correlated LPS length with forces of adhesion (F_{adh}). The goal of this study was to characterize the relationship between *E. coli* adhesion and LPS properties.

MATERIALS AND METHODS

Cultures

Eight *E. coli* strains with different LPS structures were used, including three control strains that lacked O-antigens (Table 1). Cultures were short-term stored (<2 weeks) on Luria Broth Agar (LBA) plates and grown in Luria Broth (LB) at 37°C until mid-exponential phase. Cells were washed three times by centrifugation for 10 min with sterile 0.01 M phosphate buffered saline + 0.138 M NaCl + 0.0027 M KCl pH 7.4 (PBS).

Bacterial attachment to glass slides for AFM measurements

Glass slides were rinsed with ultrapure water (18.2 MΩ cm resistivity and <10 ppb total organic carbon, Millipore Milli-Q plus, Billerica, MA, USA), followed by sonication for 15 min. Slides were immersed in 3:1 (v/v) HCl/HNO_3 solution for 30 min and rinsed with ultrapure water. Slides were treated with piranha solution (7:3 (v/v) H_2SO_4/H_2O_2 solution) for 30 min followed by rinsing with ultrapure water. Glass slides were immersed in 30% 3-aminopropyltrimethoxysilane in methanol (Sigma–Aldrich) and rinsed with methanol and ultrapure water.

A 10 ml vial of bacterial solution (1×10^9 cells/ml) was combined with 300 μl of 100 mM 1-ethyl-3-(3-dimethylaminopropyl) carbodimide hydrochloride (pH 5.5, EDC, Pierce). The vial was agitated for 10 min. Following EDC treatment, 300 μl of 40 mM *N*-hydroxysulfosuccinimide (pH 7.5, Sulfo-NHS, Pierce) was combined with the bacterial solution for 10 min. Bacterial solution was added to glass slides and agitated at 40 rpm for 10–12 h to promote bacterial lawn formation. We previously published a detailed schematic of the bacterial bonding process (Liu and Camesano, 2007). EDC/NHS will bind to amine-group terminations on the bacterial LPS. Functional amino groups on the bacterial LPS that do not take part in binding to the carboxyl groups covering the glass will quickly revert back to their original state since intermediate products are unstable (Wissink *et al.*, 2000). Therefore, the bacterial LPS exposed to the AFM probe will be in an intact natural state and will not affect the ζ potential of the bacterium.

Table 1. *E. coli* strains used in present study

Strain	Source
E. coli HB101 (ATCC 33694)	ATCC[a]
E. coli K12 (ATCC 29425)	NSRDEC[b]
E. coli ML35 (ATCC 43827)	NSRDEC
E. coli O113:H4	Health Canada
E. coli O113:H21	University Arizona; ECOR #30[c]
E. coli O157:H7 (ATCC 43895)	ATCC
E. coli O157:H12	Health Canada
E. coli O157:H16	Health Canada

[a] American Type Culture Collection.
[b] US Army Natick Soldier Research, Development and Engineering Center.
[c] *Escherichia coli* Reference Collection.

Atomic force microscopy

Silicon nitride probes were immersed in 100% ethanol for 1 h followed by UV treatment (365 nm) to remove organic films. Spring constants of the silicon nitride cantilevers (tip radius = 20–60 nm; Veeco Instruments Inc., Santa Barbara, CA) were measured using a thermal calibration method, and were found to be 0.07 ± 0.01 N/m (Matei *et al.*, 2006). The AFM was a Digital Instruments Dimension 3100 with a Nanoscope III Controller (Santa Barbara, CA).

Images of the bacteria were captured prior to force measurements in intermittent contact mode in PBS to mimic physiological conditions (Figure 1). The bacteria that we analyzed were single cells and bacteria that were closely packed were not analyzed. The scan rate was 1.0 Hz and images were captured with 512 × 512 resolution. For each strain, 10 cells were probed, and five force profiles were captured for each one; hence 50 force curves were analyzed per condition. Examples of force cycles for *E. coli* HB101, *E. coli* O113:H4, and *E. coli* O157:H7 are given in Figure 2. Each force profile contained 512 data points. F_{adh} was measured from the retraction portions of the force cycles. Loading rate, which is the product of the spring constant and retraction velocity, was 864 nN/s and was held constant for all experiments. Prior to and following a force cycle on a bacterium,

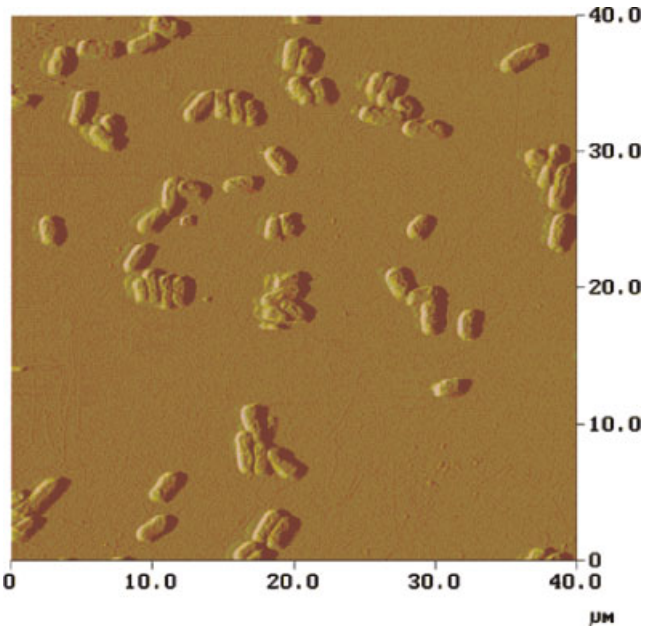

Figure 1. Example of *E. coli* O157:H7 immobilized to a functionalized glass slide using the EDC/NHS treatment in PBS. Force cycles are conducted by centralizing the AFM probe over a bacterium that is immobilized. Five force profiles were recorded per bacterium and 10 bacteria were probed per strain.

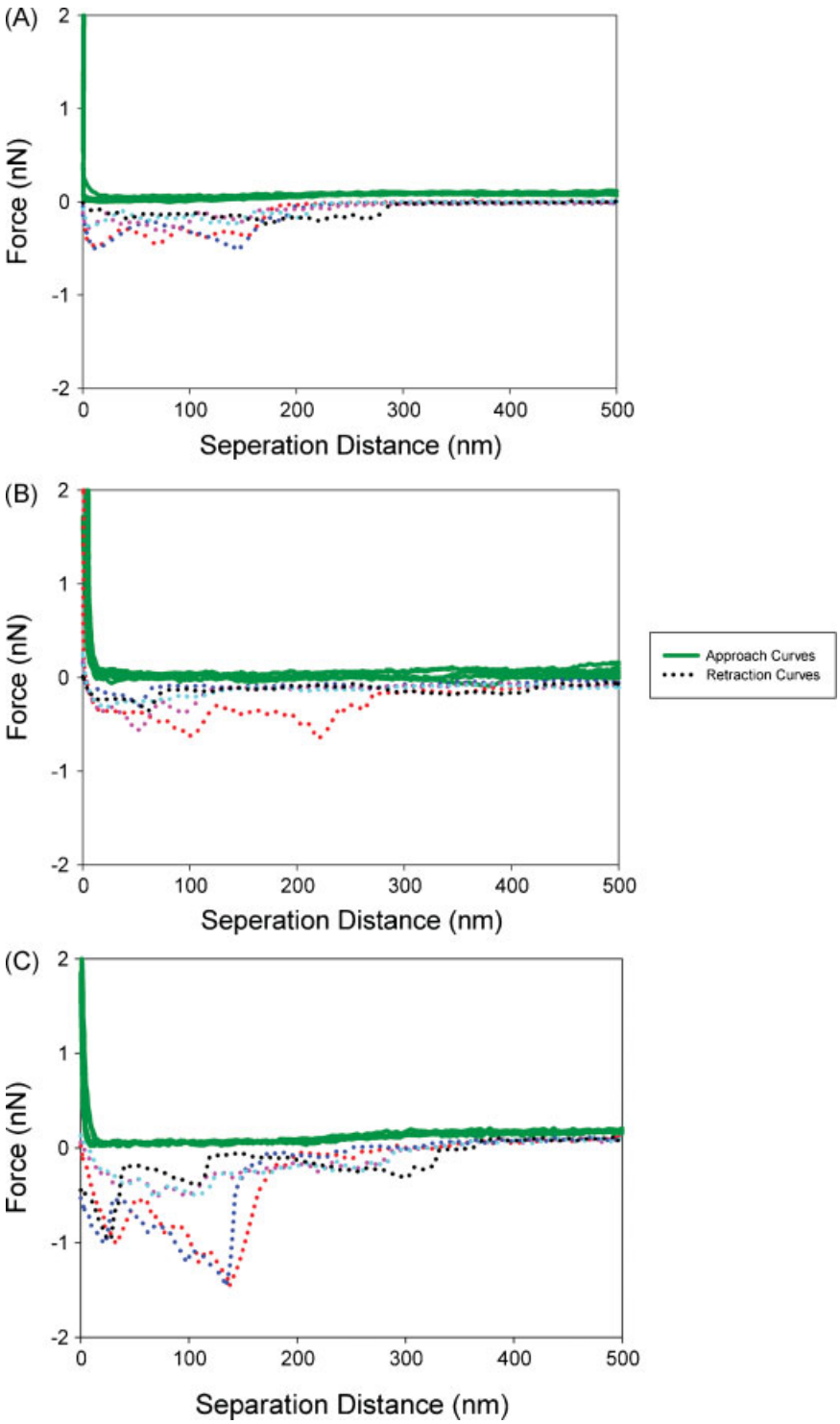

Figure 2. Representative force cycles on three *E. coli* strains. Break-off events occur as the retracting probe overcomes adhesion forces. Pull-off length of LPS is significantly longer than what is measured with steric modeling since LPS can stretch longer than the contour length and clusters of molecules may be probed in a single pull-off event. (A) Five force cycles on an *E. coli* HB101 cell. (B) Five force cycles on an *E. coli* O113:H4 cell. (C) Five force cycles on an *E. coli* O157:H7 cell.

force measurements were made on a clean glass slide. If a single sharp adhesion minimum was observed in the approach profile at ~0–5 nm, then the probe was considered clean and could be used for subsequent experiments.

Approach curves were modeled to quantify steric interactions, using the models of Alexander (1977) and de Gennes (1987), as modified for AFM analysis (Butt *et al.*, 1999).

$$\ln\left(\frac{F}{F_o}\right) = \frac{-2\pi}{L}\delta \quad (1)$$

where F is the steric force, F_0 the force at zero separation, L a fitting parameter for representing equilibrium polymer brush

length, which will be denoted as LPS length, and δ is the tip-sample separation.

Statistical analyses

Statistical software packages from SigmaStat (vs. 2.03) and SAS® were used to analyze the AFM data. One-way ANOVA tests were used to compare mean forces of adhesion of control strains with O-antigen expressing strains.

ζ potentials

The ζ potential for each of the eight strains was measured using a ζ potential analyzer (Zetasizer Nano ZS; Malvern Instruments, Worcestershire, UK). *E. coli* were washed three times in water to remove growth media and salts. Cells were diluted to 1×10^8 cells/ml and injected in a folded capillary cell (DTS1060; Malvern Instruments). Three sets of at least 10 measurements (100 max) were conducted to ensure reproducibility. Using the Smoluchowski equation (Smoluchowski, 1916), the electrophoretic motilities and surface potentials were converted to ζ potentials to characterize the negative charge of the bacterium.

RESULTS

Steric model on *E. coli* to determine LPS length

The steric model was applied to the approach curves (Figure 3A) and an $R^2 > 0.90$ was achieved for all data sets (Figure 3B). The LPS lengths were the shortest for the three strains that lacked the O-antigen: HB101, K12, and ML35. The average LPS length of the control strains was 3.5 nm, which is attributed to the lipid A and core polysaccharide molecules. Averaged equilibrium polymer lengths for control strains were statistically similar based on the ANOVA test ($p = 0.92$) (Table 2).

By applying steric modeling to the approach curves of the five *E. coli* strains that express O-antigen, we could make quantitative comparisons based on LPS characteristics. LPS lengths varied from 17 to 37 nm for strains with O-antigens (Table 2). When we further considered one serotype, we found that *E. coli* with the same O-antigen (in terms of sugar composition) had significantly different LPS lengths. For example, O157:H7, O157:H12, and O157:H16 expressed LPS lengths that were significantly different

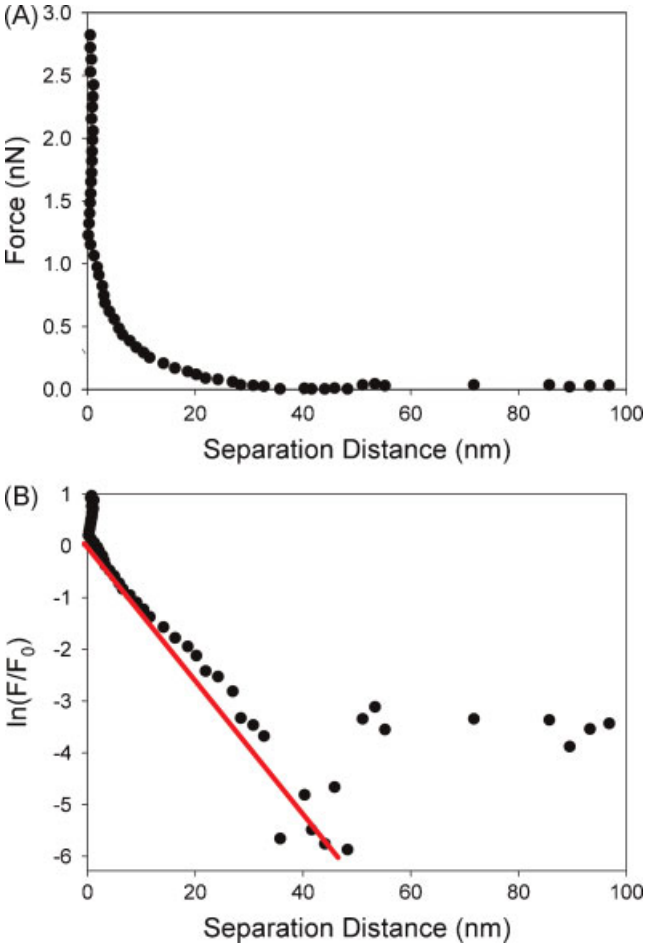

Figure 3. Representative steric modeling for *E. coli* O157:H7. (A) Representative approach curve on a single bacterium (linear scale). The repulsive event as the AFM probe contacts the LPS is detected by the AFM probe 49 nm from the rigid bacterial membrane. During this event, the AFM probe is repelled upward before overcoming steric repulsion. (B) Steric modeling of approach curve, with slope of fitting line equal to $-2\pi/L$ (natural log scale for *y*-axis). $R^2 > 0.90$ for all steric modeling. Based on example, LPS length is 49 nm.

Table 2. Bacterial LPS properties measured from steric modeling

Strain	Equilibrium length (nm)	Core type[a]	F_{adh} (nN)	Linear trend (F_{adh} versus LPS length)
HB101[b]	**5 ± 3**	**K12**	**0.4 ± 0.1**	**Control strains $y = 0.79–0.08x$, $R^2 = 0.30$**
K12	**3 ± 2**	**K12**	**0.5 ± 0.2**	
ML35	**3 ± 2**	**K12**	**0.7 ± 0.4**	
O113:H4	17 ± 10	R3	0.6 ± 0.6	O-antigen strains $y = 0.07 + 0.02x$, $R^2 = 0.84$
O113:H21	37 ± 9	R1	1.0 ± 0.4[c]	
O157:H7	30 ± 13	R3	0.7 ± 0.4	All strains $y = 0.42 + 0.01x$, $R^2 = 0.54$
O157:H12	25 ± 9	R2	0.6 ± 0.2	
O157:H16	19 ± 6	R2	0.5 ± 0.2	

[a] Core types from Amor *et al.* (2000).
[b] Bold text represents control K12 strains that do not express the O-antigen.
[c] Significantly different from all other strains in study ($p < 0.05$).

Journal of Molecular Recognition

from one another ($p < 0.05$). The two O113 serotypes had LPS lengths of 17 ± 10 nm (for O113:H4) and 37 ± 9 nm (for O113:H21), and these values were statistically different from one another ($p < 0.05$). Further, LPS lengths of each of the control strains were significantly shorter compared to all O-antigen expressing strains ($p < 0.05$).

E. coli adhesive forces

Each *E. coli* strain had a different F_{adh} with the silicon nitride probe. Even for the control strains, there were some differences in the adhesion forces they exhibited for the AFM tip. Absolute adhesion forces for HB101, K12, and ML35 were 0.4 ± 0.1, 0.7 ± 0.4, and 0.5 ± 0.2 nN, respectively (Table 2). The adhesion force of *E. coli* ML35 with silicon nitride was significantly higher than the adhesion of either HB101 or K12 to the probe ($p < 0.05$).

Of the five O-antigen expressing strains, only *E. coli* O113:H21 exhibited adhesion forces that were significantly greater than the average of the control strains (Table 2). While O157:H7 and O157:H12 had F_{adh} values that were similar to each other, F_{adh} were significantly less for O157:H16 ($p < 0.05$) (Table 2). The two O113 serotype strains did not have similar F_{adh} values, with O113:H21 exhibiting significantly greater F_{adh} with silicon nitride than O113:H4 ($p < 0.05$).

Effect of core types

The core type had little effect on F_{adh}, with F_{adh} values being statistically similar for K12, R2, and R3 cores (Figure 4). The adhesion seemed higher for the strain with an R1 core (O113:H21), but we cannot make this conclusion since we only examined one bacterial strain with this core type (Table 2). The control strains that express the K12 core had equilibrium polymer lengths that were conserved and significantly shorter than bacteria of the R1, R2, and R3 core types ($p < 0.05$). However, R1, R2, and R3 strains also expressed the O-antigen that we associated with the longer LPS.

Correlating LPS length to F_{adh}

There was no correlation between fitted LPS length and F_{adh} with silicon nitride for any of the control strains (Figure 5). For strains O113 and O157, F_{adh} the maximum adhesion force per force curve correlated positively with LPS length (Figures 6 and 7). The strongest correlations were observed for O157:H7 and O157:H12 ($R^2 > 0.90$). Strain O157:H16, which expressed the shortest LPS, had a weak correlation between LPS length and F_{adh} ($R^2 = 0.54$).

When we grouped strains according to whether they expressed the O-antigen, average LPS lengths correlated well with average F_{adh} for O-antigen expressing strains ($R^2 = 0.84$) (Table 2). However, when no O-antigen was present, the correlation was poor ($R^2 = 0.30$).

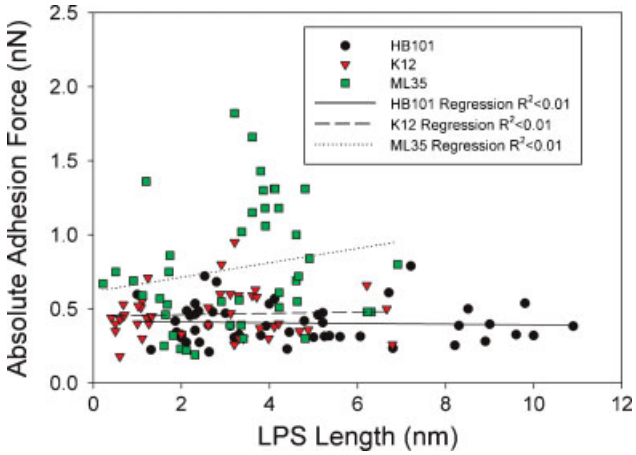

Figure 5. LPS calculated lengths compared to absolute adhesion forces per force cycle. R^2 values represent goodness-of-fit for linear regression of *E. coli* HB101, K12, and ML35.

Correlating ζ potential with LPS lengths

Control strains were the most negatively charged, at < -40 mV (Figure 8). There was no clear trend of ζ potentials versus LPS length for control strains. However, when considering the relation of *E. coli* LPS length to ζ potential, we found a positive linear correlation ($R^2 = 0.92$). *E. coli* O113:H4 and O157:H16, which had

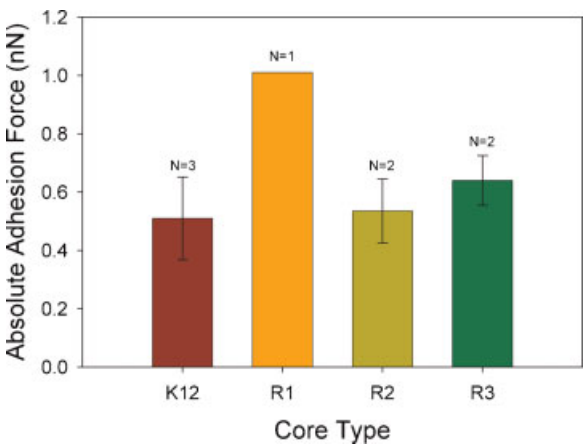

Figure 4. AFM adhesion forces on silicon nitride probes. F_{adh} were averaged for strains containing the same core types.

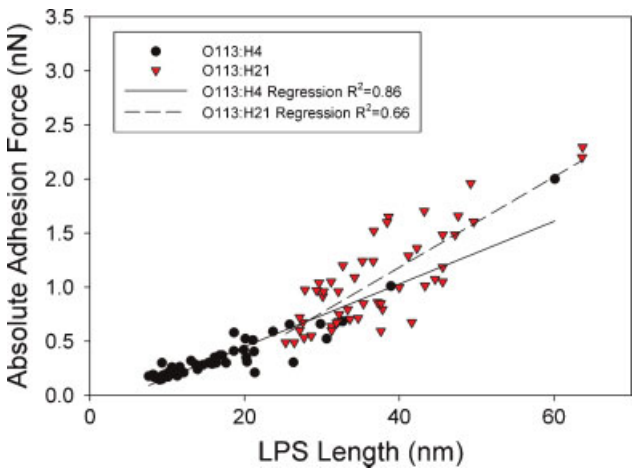

Figure 6. LPS calculated lengths compared to absolute adhesion forces per force cycle. R^2 values represent goodness-of-fit for linear regression of *E. coli* O113:H4 and O113:H21.

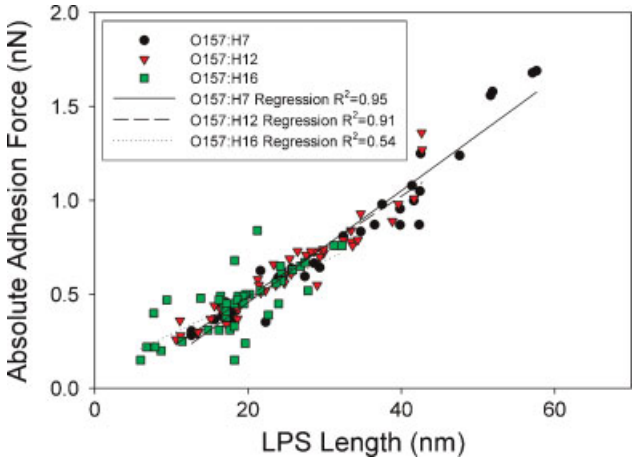

Figure 7. LPS calculated lengths compared to absolute adhesion forces per force cycle. R^2 values represent goodness-of-fit for linear regression of *E. coli* O157:H7, O157:H12, and O157:H16.

the shortest LPS length, were comparable in terms of their ζ potentials. Equilibrium polymer lengths for *E. coli* O157:H7 and O113:H21 differed by 7 nm and both were $\geq$30 nm. These were the only strains with ζ potentials >-15 mV (Figure 6). ζ potential was independent of O-antigen or core oligosaccharide composition.

DISCUSSION

Relationship between LPS length and adhesion force for control strains

From the steric modeling, we calculated LPS lengths for the control strains that are consistent with literature predictions. For example, Lee estimated the lipid A region to be ~2.3 nm (Lee, 2003), with the length due to fatty acids of C12, C14, C16, and C18 (Rietschel *et al.*, 1994). The combination of the lipid A plus inner, and outer cores was 4.4 nm for *E. coli* and *Salmonella typhimurium* (Kastowsky *et al.* 1992).

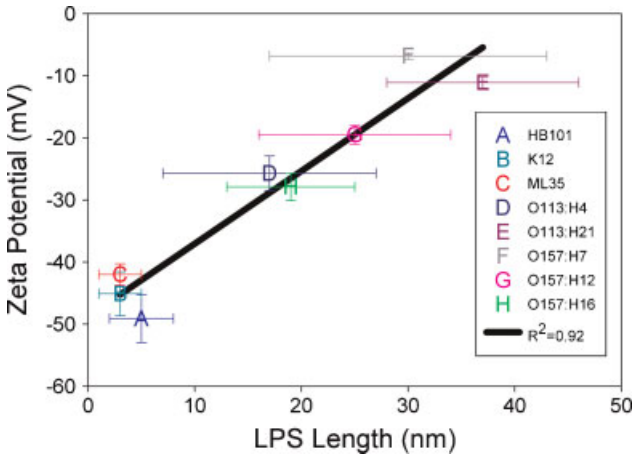

Figure 8. ζ potentials for the eight *E. coli* strains measured in ultrapure water.

The LPS lengths we calculated for the control strains were close to these values, but were somewhat shorter than expected. Although our prior work has shown that steric repulsion dominates bacterial AFM approach curves, electrostatic interactions can also influence LPS conformation (Camesano and Logan, 2000; Abu-Lail and Camesano, 2003b). Lower ionic strength solutions correlate to increased steric repulsion (Johnson *et al.*, 2005). For example, an ionic strength increases from 0.01 to 0.1 M reduced bacterial polymer length four-fold due to coiling of bacterial surface molecules (Abu-Lail and Camesano, 2003a). At the ionic strengths used in the present study, the reported LPS length values may also reflect the coiling of biopolymers on the bacterial surface. Thus, if polymers were slightly coiled, we may be underpredicting their lengths. However, the same ionic strength was used for all experiments, so this coiling effect would have been constant for all strains.

We do not expect any differences in the LPS structure or core for the three K12 strains, and the LPS lengths calculated via the steric model were similar. However, differences in the adhesion forces with silicon nitride were observed among the three K12 strains. These differences may have been influenced by the presence of other biomacromolecules, lipids, and phospholipids on the bacterial surfaces. Normally, the O-antigen masks underlying proteins in the outer membrane (Jucker *et al.*, 1997; Walker *et al.*, 2004). However, since the control strains lack the O-antigen, the adhesion force values that we observed may also have been related to other biomacromolecules and underlying lipids. ζ potential measurements demonstrated that *E. coli* not expressing the O-antigen have a more negative charge. This is not necessarily due to control strains expressing more phospholipids, but rather could be due to the O-antigen providing shielding of electrostatic double-layer interactions (Walker *et al.*, 2004).

In addition, ML35 produces the enzyme β-galactosidase, which acts as a phenotype marker (Guven *et al.*, 2005). ML35 releases larger quantities of β-galactosidase following membrane penetration (Guven *et al.*, 2005). The presence of β-galactosidase may have enhanced adhesion with the silicon nitride probe compared to the other control strains, although this would need to be confirmed with other experiments.

Relationship between adhesion forces and LPS lengths for O-antigen expressing strains

Bacteria are classified in terms of repeating chains of their O-antigen, capsular composition, and flagella antigens (Hitchcock *et al.*, 1986), but the number of repeating O-antigen units is not part of the serotype classification and may vary greatly within a population of bacteria. The length of a single O-antigen unit was estimated to be ~1.0–1.3 nm (Kastowsky *et al.*, 1992; Murray *et al.*, 2006). *E. coli* equilibrium LPS lengths were O113:H21 > O157:H7 > O157:H12 > O157:H16 > O113:H4. The O157 strains did not significantly differ from one another in terms of average adhesion forces with silicon nitride. *E. coli* O113:H21 was significantly more adhesive to silicon nitride than all other strains, which apparently was due to the longer LPS lengths observed for this strain.

The O-antigen is a highly variable structure that enables *E. coli* attachment to a host cell or biomaterial using specific ligand–receptor bonding. For instance, *E. coli* O113 and O157 can adhere well to the intestinal tract and fresh produce (Manges *et al.*, 2001).

Journal of Molecular Recognition

Our results suggest differing sections of the LPS-mediated adhesion to silicon nitride for control and O-antigen expressing strains. With the exception of O113:H21 F_{adh} was almost the same for control and O-antigen expressing strains. However, F_{adh} was independent of core length for control strains, while an increasing number of O-antigen units present caused F_{adh} to increase. Underlying proteins and lipids may have adhered to the silicon nitride probe in the case of the control strains (Jucker *et al.*, 1997). Electrostatic charges of *E. coli* are partially influenced by negatively charged lipids and phospholipids, and these charges may have been shielded in the case of O-antigen expressing strains (Walker *et al.*, 2004). Therefore, the mechanisms governing F_{adh} for control strains may be electrostatic interactions, while O-antigen bonds to silicon nitride probes with hydrogen bonding.

LPS binding may have been governed by the number of O-antigen units interacting with the silicon nitride. Even the shortest calculated O-antigen of 13 nm for O113:H4 (calculated by subtracting LPS length of O113:H4 with averaged LPS length of control strains) may have blocked the effects of underlying proteins and lipids. The O-antigen of O113:H4 may be too short to adhere as well to silicon nitride as that of O113:H21. Murray *et al.* (2006) found 16–35 units (16–46 nm) of the O-antigen expressed by *Salmonella enterica* to be most efficient for macrophage cells to adhere to and uptake bacteria. This study found a similar trend in that ~15–35 units of the O-antigen on average were most efficient for *E. coli* adhesion to silicon nitride (Table 2). However, based on our AFM force measurements, longer O-antigen molecules extending >50 nm had the strongest adhesion with the AFM probe (Figures 4 and 5).

E. coli O113 is an enterohemorrhagic strain (EHEC) due to expression of Shiga-like toxins (Paton *et al.*, 1999). Adhesion to host cells in the intestinal tract is a precondition to symptoms of dysentery (Yu and Kaper, 1992; Phillips *et al.*, 2000). It is therefore possible that increased adhesion has contributed to this pathogen's ability to infect host tissue. However, whether LPS length can be used to predict *E. coli* virulence would require further study.

Comparison of F_{adh} based on O-antigen composition

The trend of increasing adhesion forces for bacteria expressing longer LPS may indicate that more sugars of the O-antigen chain were binding to the silicon nitride. Comparing adhesion profiles in Figures 4 and 5, O113 and O157 bind more efficiently when they express longer LPS, but we cannot distinguish F_{adh} based on sugar compositions of the O-antigens or core groups. SiO_2 forms

Table 3. O-antigens and core oligosaccharides for pathogenic strains

O113:H4 R3 Core[1]

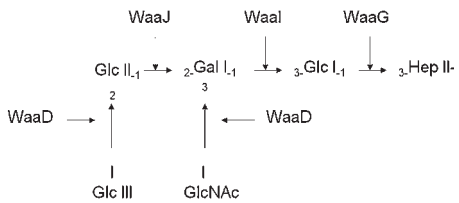

O113:H21 R1 Core

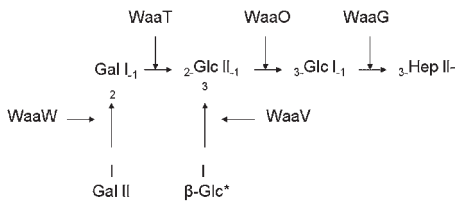

O113 O-antigen

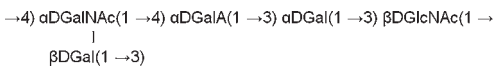

O157:H12 & O157:H16 R2 Core

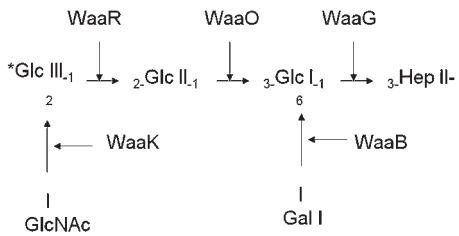

O157 O-antigen

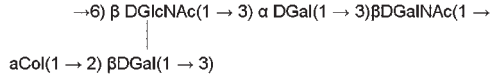

Fuc, Fucose; Gal, Galactose; Glc, Glucose; Hep, Heptose; GalNAc, *N*-acetylgalactosamine; GlcNAc, *N*-acetylglucosamine; RhaNAc, *N*-acetyl-L-rhamnosamine; Rha, Rhamnose. *Represents point of attachment between core oligosaccharide and O-antigen. [1]Same for O157:H7.

when silicon nitride is oxidized (Riley, 2000). About 5×10^6 silanol groups per μm^2 are present on the surface of SiO_2 (Zhuravlev, 1987). Hydrogen bonding with biomolecules and inorganic molecules has been proposed as an important function of the O-antigen. The hydroxyl group of silanol can mediate hydrogen bonds with the O-antigen when silica is present (Jucker *et al.*, 1997). Binding to inorganic molecules such as silicon nitride may be highly dependent on the number of hydrogen bonds that can form. A previous study on isolated O-antigens showed that hydrogen bonding was important in controlling O-antigen adhesion to inorganic molecules such as TiO_2, SiO_2, and Al_2O_3 (Jucker *et al.*, 1997).

So far, it has not been possible to relate O-antigen chemical composition to adhesion, even though sugars bind through hydrogen bonds (Stubenrauch, 2001). For example, the O157 O-antigen is comprised of *N*-acetyl-L-rhamnosamine, fucose, glucose, and *N*-acetylgalactosamine, while each chain unit for O113 contains three galactose sugars, *N*-acetylgalactosamine, and *N*-acetylglucosamine (Table 3). F_{adh} was significantly different between O113:H4/O113:21 and O157:H7/O157:H16, while LPS lengths correlated well to F_{adh} for all O-antigen expressing strains. No correlations were established between O-antigen composition and adhesion to minerals such as silica in a prior study on isolated bacterial O-antigens (Jucker *et al.*, 1998).

Comparison of F_{adh} based on core type

The core oligosaccharide serves as a bridge between the highly variable O-antigen and lipid A, and its role in adhesion has never been investigated. There are only five core structures for *E. coli*: K12, R1, R2, R3, and R4. The O-antigen is not conserved to a particular core structure. For instance, O113:H4 has the R3 core while O113:H21 has an R1 core. Strain O157:H7 has an R3 core, while O157:H12 and O157:H16 have the R2 core. The R2 and K12 cores share backbones, with differences found in the terminal side chains (Heinrichs *et al.*, 1998).

Based on our experiments, we did not find clear relations between core oligosaccharide and LPS length or adhesion force. For example, O113:H4 and O157:H7 each have an R3 core, while LPS length for O157:H7 was double that of O113:H4. Strains possessing the R2 cores and R3 core were indistinguishable in terms of LPS length or adhesion forces.

Strain O113:H21 has an R1 core, and this strain behaved very differently from O113:H4 in terms of adhesion force. Since both strains express the same O-antigen, the core group may have been a contributing factor to the observed differences and adhesion forces were significantly different between O113:H4 and O113:H21. However, based on the strong correlation between F_{adh} and polymer length, we suggest that the core polysaccharide may be less important in mediating initial interaction with inorganic substrates such as silicon nitride.

CONCLUSION

E. coli strains O157 and O113 are pathogenic strains that are similar based on their involvement in food and water contamination and cause the same human intestinal diseases (Manges *et al.*, 2001). F_{adh} between silicon nitride and O157 or O113 did not correlate well to O-antigen or core group chemical composition. However, physical properties of the LPS were important. We observed stronger F_{adh} for strains with longer LPS, when the O-antigen was being expressed. For strains without O-antigens, there were no correlations between F_{adh} and LPS length. O-antigen expressing strains apparently adhered to the probes through hydrogen bonds. Control strains were also more influenced by electrostatic interactions. This study suggests that LPS length is an important prediction of bacterial adhesion forces for O-antigen expressing strains.

Acknowledgements

We are grateful to Mr Soares of the US Army Natick Soldier Research, Development, and Engineering Center for contributing *E. coli* K12 and ML35, Dr Ochman of the University of Arizona for *E. coli* O113:H21, and Dr Ziebel of Health Canada for *E. coli* O113:H4, O157:H12, and O157:H16. We also appreciate useful discussions with Ms Pinzón-Arango. We thank the National Science Foundation (BES 0238627) for partial support of this research.

REFERENCES

Abu-Lail NI, Camesano TA. 2003a. Role of ionic strength on the relationship of biopolymer conformation, DLVO contributions, and steric interactions to bioadhesion of Pseudomonas putida KT2442. *Biomacromolecules.* **4**: 1000–1012.

Abu-Lail NI, Camesano TA. 2003b. Role of lipopolysaccharides in the adhesion, retention, and transport of *Escherichia coli* JM109. *Environ. Sci. Technol.* **37**: 2173–2183.

Alexander S. 1977. Adsorption of chain molecules with a polar head a scaling description. *J. Phys.* **38**: 983–987.

Amor K, Heinrichs DE, Frirdich E, Ziebell K, Johnson RP, Whitfield C. 2000. Distribution of core oligosaccharide types in lipopolysaccharides from *Escherichia coli*. *Infect. Immun.* **68**: 1116–1124.

Bell BP, Goldoft M, Griffin PM, Davis MA, Gordon DC, Tarr PI, Bartleson CA, Lewis JH, Barrett TJ, Wells JG, Baron R, Kobayashi J. 1994. A multistate outbreak of *Escherichia coli* O157: H7-associated bloody diarrhea and hemolytic uremic syndrome from hamburgers. The Washington experience. *JAMA* **272**: 1349–1353.

Besser RE, Lett SM, Weber JT, Doyle MP, Barrett TJ, Wells JG, Griffin PM. 1993. An outbreak of diarrhea and hemolytic uremic syndrome from *Escherichia coli* O157: H7 in fresh-pressed apple cider. *JAMA* **269**: 2217–2220.

Bettelheim KA, Breadon A, Faiers MC, O'Farrell SM, Shooter RA. 1974. The origin of O serotypes of *Escherichia coli* in babies after normal delivery. *J. Hyg.* **72**: 67–70.

Butt HJ, Kappl M, Mueller H, Raiteri R, Meyer W, Ruhe J. 1999. Steric forces measured with the atomic force microscope at various temperatures. *Langmuir* **15**: 2559–2565.

Camesano TA, Logan BE. 2000. Probing bacterial electrosteric interactions using atomic force microscopy. *Environ. Sci. Technol.* **34**: 3354–3362.

Caroff M, Karibian D. 2003. Structure of bacterial lipopolysaccharides. *Carbohydr. Res.* **338**: 2431–2447.

Ciftcioglu G, Arun OO, Vural A, Aydin A, Aksu H. 2008. Survival of *Escherichia coli* O157: H7 in minced meat and hamburger patties. *J. Food Agric. Environ.* **6**: 24–27.

Dean-Nystrom EA, Bosworth BT, Cray WC Jr, Moon HW. 1997. Pathogenicity of *Escherichia coli* O157: H7 in the intestines of neonatal calves. *Infect. Immun.* **65**: 1842–1848.

de Gennes PG. 1987. Polymers at an interface—a simplified view. *Adv. Colloid Interface Sci.* **27**: 189–209.

Franco AV, Liu D, Reeves PR. 1998. The Wzz (Cld) protein in *Escherichia coli*: amino acid sequence variation determines O-antigen chain length specificity. *J. Bacteriol.* **180**: 2670–2675.

Goldman RC, Hunt F. 1990. Mechanism of O-Antigen distribution in lipopolysaccharide. *J. Bacteriol.* **172**: 5352–5359.

Griffin PM, Tauxe RV. 1991. The epidemiology of infections caused by *Escherichia coli* O157 H7, other enterohemorrhagic *Escherichia coli*, and the associated hemolytic uremic syndrome. *Epidemiol. Rev.* **13**: 60–98.

Guven K, Yolcu M, Gul-Guven R, Erdogan S, De Pomerai D. 2005. The effects of organic pesticides on inner membrane permeability in *Escherichia coli* ML35. *Cell Biol. Toxicol.* **21**: 73–81.

Heinrichs DE, Monteiro MA, Perry MB, Whitfield C. 1998. The assembly system for the lipopolysaccharide R2 core-type of *Escherichia coli* is a hybrid of those found in *Escherichia coli* K-12 and *Salmonella enterica*. Structure and function of the R2 WaaK and WaaL homologs. *J. Biol. Chem.* **273**: 8849–8859.

Hitchcock PJ, Leive L, Makela PH, Rietschel ET, Strittmatter W, Morrison DC. 1986. Lipopolysaccharide nomenclature—past, present, and future. *J. Bacteriol.* **166**: 699–705.

Johnson CP, Fujimoto I, Rutishauser U, Leckband DE. 2005. Direct evidence that neural cell adhesion molecule (NCAM) polysialylation increases intermembrane repulsion and abrogates adhesion. *J. Biol. Chem.* **280**: 137–145.

Jucker BA, Harms H, Hug SJ, Zehnder AJB. 1997. Adsorption of bacterial surface polysaccharides on mineral oxides is mediated by hydrogen bonds. *Colloids Surf. B* **9**: 331–343.

Jucker BA, Harms H, Zehnder AJB. 1998. Polymer interactions between five gram-negative bacteria and glass investigated using LPS micelles and vesicles as model systems. *Colloids Surf. B* **11**: 33–45.

Karrasch S, Hegerl R, Hoh JH, Baumeister W, Engel A. 1994. Atomic-force microscopy produces faithful high-resolution images of protein surfaces in an aqueous environment. *Proc. Natl Acad. Sci. U. S. A.* **91**: 836–838.

Kastowsky M, Gutberlet T, Bradaczek H. 1992. Molecular modelling of the three-dimensional structure and conformational flexibility of bacterial lipopolysaccharide. *J. Bacteriol.* **174**: 4798–4806.

Lee AG. 2003. Lipid-protein interactions in biological membranes: a structural perspective. *Biochim. Biophys. Acta* **1612**: 1.

Liu Y, Camesano TA. 2007. Immobilizing Bacteria for Atomic Force Microscopy Imaging or Force Measurements in Liquids. *ACS Symp. Ser.* **984**: 163–188.

Liu Y, Strauss J, Camesano TA. 2008. Adhesion forces between *Staphylococcus epidermidis* and surfaces bearing self-assembled monolayers in the presence of model proteins. *Biomaterials* **29**: 4374.

Maki DG. 2006. Don't eat the spinach—controlling foodborne infectious disease. *N. Engl. J. Med.* **355**: 1952–1955.

Makin SA, Beveridge TJ. 1996. The influence of A-band and B-band lipopolysaccharide on the surface characteristics and adhesion of *Pseudomonas aeruginosa* to surfaces. *Microbiology* **142**: 299–307.

Manges AR, Johnson JR, Foxman B, O'Bryan TT, Fullerton KE, Riley LW. 2001. Widespread distribution of urinary tract infections caused by a multidrug-resistant *Escherichia coli* clonal group. *N. Engl. J. Med.* **345**: 1007–1013.

Matei GA, Thoreson EJ, Pratt JR, Newell DB, Burnham NA. 2006. Precision and accuracy of thermal calibration of atomic force microscopy cantilevers. *Rev. Sci. Instrum.* **77**: 083703.

Moller C, Allen M, Elings V, Engel A, Muller DJ. 1999. Tapping-mode atomic force microscopy produces faithful high-resolution images of protein surfaces. *Biophys. J.* **77**: 1150–1158.

Murray GL, Attridge SR, Morona R. 2006. Altering the length of the lipopolysaccharide O-antigen has an impact on the interaction of *Salmonella enterica* and *Serovar typhimurium* with macrophages and complement. *J. Bacteriol.* **188**: 2735–2739.

Nataro JP, Kaper JB. 1998. Diarrheagenic *Escherichia coli*. *Clin. Microbiol. Rev.* **11**: 142–201.

Parma AE, Sanz ME, Blanco JE, Blanco J, Vinas MR, Blanco M, Padola NL, Etcheverria AI. 2000. Virulence genotypes and serotypes of verotoxigenic *Escherichia coli* isolated from cattle and foods in Argentina - Importance in public health. *Eur. J. Epidemiol.* **16**: 757–762.

Paton AW, Woodrow MC, Doyle RM, Lanser JA, Paton JC. 1999. Molecular characterization of a shiga toxigenic *Escherichia coli* O113: H21 strain lacking eae responsible for a cluster of cases of hemolytic-uremic syndrome. *J. Clin. Microbiol.* **37**: 3357–3361.

Phillips AD, Navabpour S, Hicks S, Dougan G, Wallis T, Frankel G. 2000. Enterohaemorrhagic *Escherichia coli* O157: H7 target Peyer's patches in humans and cause attaching/effacing lesions in both human and bovine intestine. *Gut* **47**: 377–381.

Rietschel ET, Kirikae T, Schade FU, Mamat U, Schmidt G, Loppnow H, Ulmer AJ, Zahringer U, Seydel U, Di Padova F. 1994. Bacterial endotoxin: molecular relationships of structure to activity and function. *FASEB J.* **8**: 217–225.

Riley FL. 2000. Silicon nitride and related materials. *J. Am. Ceram. Soc.* **83**: 245–265.

Schromm AB, Brandenburg K, Loppnow H, Moran AP, Koch MHJ, Rietschel ET, Seydel U. 2000. Biological activities of lipopolysaccharides are determined by the shape of their lipid A portion. *Eur. J. Biochem.* **267**: 2008–2013.

Sheng H, Lim JY, Watkins MK, Minnich SA, Hovde CJ. 2008. Characterization of an *Escherichia coli* O157: H7 O antigen deletion mutant and its effect on persistence in mouse intestine and colonization at the bovine terminal rectal mucosa. *Appl. Environ. Microbiol.* **74**: 5015–5022.

Smoluchowski M. 1916. Drei vortraege ueber diffusion, brownsche molekularbewegun und koagulation von kolloidtielchen. *Phys. Zeits.* **37**: 557–570.

Stenutz R, Weintraub A, Widmalm G. 2008. E. coli O-antigen Database. Retrieved 12.8.07, from http://www.casper.organ.su.se/ECODAB/

Strachan NJC, Dunn GM, Locking ME, Reid TMS, Ogden ID. 2006. Escherichia coli O157: burger bug or environmental pathogen? *Int. J. Food Microbiol.* **112**: 129.

Stubenrauch C. 2001. Sugar surfactants—aggregation, interfacial, and adsorption phenomena. *Curr. Opin. Colloid Interface Sci.* **6**: 160.

Sumihiro Hase ETR. 1976. Isolation and analysis of the lipid A backbone. *Eur. J. Biochem.* **63**: 101–107.

Tang KH, Guo H, Yi W, Tsai MD, Wang PG. 2007. Investigation of the conformational states of Wzz and the Wzz #183;O-antigen complex under near-physiological conditions. *Biochemistry* **46**: 11744–11752.

Taylor ES, Lower SK. 2008. Thickness and surface density of extracellular polymers on *Acidithiobacillus ferrooxidans*. *Appl. Environ. Microbiol.* **74**: 309–311.

Tomme P, Creagh AL, Kilburn DG, Haynes CA. 1996. Interaction of polysaccharides with the N-terminal cellulose-binding domain of Cellulomonas fimi CenC.1. Binding specificity and calorimetric analysis. *Biochemistry* **35**: 13885–13894.

Touhami A, Nysten B, Dufrene YF. 2003. Nanoscale mapping of the elasticity of microbial cells by atomic force microscopy. *Langmuir* **19**: 4539–4543.

Uhlich GA, Sinclair JR, Warren NG, Chmielecki WA, Fratamico P. 2008. Characterization of shiga toxin-producing *Escherichia coli* isolates associated with two multistate food-borne outbreaks that occurred in 2006. *Appl. Environ. Microbiol.* **74**: 1268–1272.

Walker SL, Redman JA, Elimelech M. 2004. Role of cell surface lipopolysaccharides in *Escherichia coli* K12 adhesion and transport. *Langmuir* **20**: 7736–7746.

Whitfield C. 1995. Biosynthesis of lipopolysaccharide O antigens. *Trends Microbiol.* **3**: 178.

Wissink MJB, van Luyn MJA, Beernink R, Dijk F, Poot AA, Engbers GHM, Beuqeling T, van Aken WG, Feijen J. 2000. Endothelial cell seeding on crosslinked collagen: Effects of crosslinking on endothelial cell proliferation and functional parameters. *Thromb. Haemost.* **84**: 325–331.

Yu J, Kaper JB. 1992. Cloning and characterization of the eae gene of enterohaemorrhagic *Escherichia coli* O157: H7. *Mol. Microbiol.* **6**: 411–417.

Zhuravlev LT. 1987. Concentration of hydroxyl-groups on the surface of amorphous silicas. *Langmuir* **3**: 316–318.